26th EPS Conf. on Contr. Fusion and Plasma Physics, Maastricht, 14 - 18 June 1999 ECA Vol.23J (1999) 1193 - 1196

Internal Transport Barriers and Turbulence Behavior in NCS Discharges on DIII–D

E.J. Doyle, T.L. Rhodes, L. Zeng, D.R. Baker,[1] K.H. Burrell,[1] J.C. DeBoo,[1] C.M. Greenfield,[1] G.R. McKee,[2] W.A. Peebles, C.L. Rettig, B.W. Rice,[3] G.M. Staebler,[1] and B.W. Stallard[3]

Dept. of Electrical Engineering and IPFR, University of California, Los Angeles, CA 90095
[1]General Atomics, San Diego
[2]University of Wisconsin-Madison
[3]Lawrence Livermore National Laboratory

I. Introduction

Very steep internal transport barriers (ITBs) have been observed in all four transport channels on DIII–D. These ITBs are the most highly localized (width ≤5 cm), simultaneous transport barriers observed on any machine to date, and have only been observed in discharges with negative central magnetic shear (NCS discharges), at power levels above ~8 MW. On DIII–D, improved ion transport with ITB operation is correlated with reduced microturbulence levels [1–3], in accord with models of turbulence and transport regulation via sheared **E**×**B** flows [1–6]. However, the improvement in electron transport reported here takes place with essentially invariant low-wavenumber (0 to ≥2 cm^{-1}) turbulence signals, suggesting that this turbulence may be unrelated to the observed improvement in electron thermal and particle transport.

On DIII–D it is much more difficult to obtain ITBs in the electron thermal and particle transport channels than in the ion thermal and angular momentum channels. ITBs in the ion thermal and angular momentum channels can be obtained with or without NCS operation [1,4,5], and at low injected power levels ~2.5 MW [5], whereas ITBs in the electron thermal and particle transport channels are only observed with strongly reversed magnetic shear (strong NCS) [5–8] and, for particle transport, at power levels above ~8 MW [8]. Transport barriers in all four transport channels have been previously observed on DIII–D [5], but with much more modest, and less localized, changes in the gradients of n_e and T_e than reported here. Steep, strongly localized gradients in n_e have also been previously observed on DIII–D, but without a strong ITB in the electron thermal channel [8], and with an ITB in T_e but not n_e [7]. The previous most localized example of simultaneous core ITBs in the electron thermal and particle transport channels was observed on JT–60U, but with a less localized transport barrier in the ion thermal channel [9]. While the improvement in core ion transport on DIII–D is believed to be understood [1–6], electron thermal transport on DIII-D typically remains anomalous, and has puzzling features [5–7]. However, there is some evidence that the electron thermal transport may be governed by high-wavenumber ETG-type turbulence [6,7], while the data presented here suggest that the electron thermal transport may be independent of low-wavenumber turbulence.

Operation with steep, highly localized ITBs such as reported in this paper is not necessarily a route to maximum plasma performance. The steep pressure gradients in these discharges commonly lead to large amplitude internal mode activity and/or loss of stability. Rather, the significance of the results presented here is that: (a) it is possible to simultaneously produce dramatically improved transport in all four transport channels and, (b) these plasmas provide an opportunity to investigate the differing mechanisms governing the formation of ITBs in the various plasma transport channels. The observation of an ITB in the electron particle transport channel in these discharges was made possible by a new profile reflectometer system specifically installed for the purpose [10]. In addition, Thomson scattering coverage has been extended to the plasma center since the start of operations in 1999 (coverage extended from $0.3 \leq \rho \leq 1.05$ to $0 \leq \rho \leq 1.05$) [11].

II. ITB Characteristics

An example of simultaneous, highly localized particle, electron and ion thermal transport barriers is shown in Fig. 1. As can be seen, the three transport barriers illustrated coincide, and are located somewhat inside the location of the minimum q value, $\rho_{q_{min}} \sim 0.5$. The highly localized (width <5 cm) regions of steep gradient are immediately apparent in the electron density and electron and ion temperature profiles. For this discharge, I_p = 1.6 MA, B_T = 2.0 T, P_{NBI} = 9.2 MW, in a double-null configuration biased towards the upper-null. As illustrated, the q profile is reversed. An example showing the time evolution of the plasma profiles (transport channels) is shown in Fig. 2, for a different discharge, though with the same plasma conditions as for Fig. 1. As shown in Fig. 2(a), an ITB is already established in the ion thermal channel by the earliest time shown (1.2 s), and as time evolves the steep gradient region extends to higher temperatures, but does so without any significant increase in gradient within the ITB region. At the same time, the profile at radii lying inside the ITB flattens ($0 \le \rho \le 0.35$). The evolution of the toroidal rotation frequency, measured for carbon impurity ions, is shown in Fig. 2(b), and closely parallels that of T_i, though the gradient region does steepen at 1.5 s. The core electron density and temperature profiles in this discharge were measured by reflectometry and ECE, respectively, as this discharge was obtained before the new tangential Thomson scattering system was installed. Reflectometers operating in the ordinary polarization (O–mode) cannot measure flat profiles, which is why the density profile at 1.2 s is not indicated for $\rho < 0.25$. Thus, at the earliest time shown, 1.2 s, the n_e and T_e profiles, Fig. 2(c) and (d), are flat in the plasma core, but do not exhibit a very steep gradient in the region where a clear ITB has already formed in the ion temperature and toroidal rotation. As time evolves, however, both the n_e and T_e profiles steepen significantly and exhibit a localized ITB in the same region as for the T_i profile. At 1.5 s, ECE T_e data are unavailable in the ITB region, due to

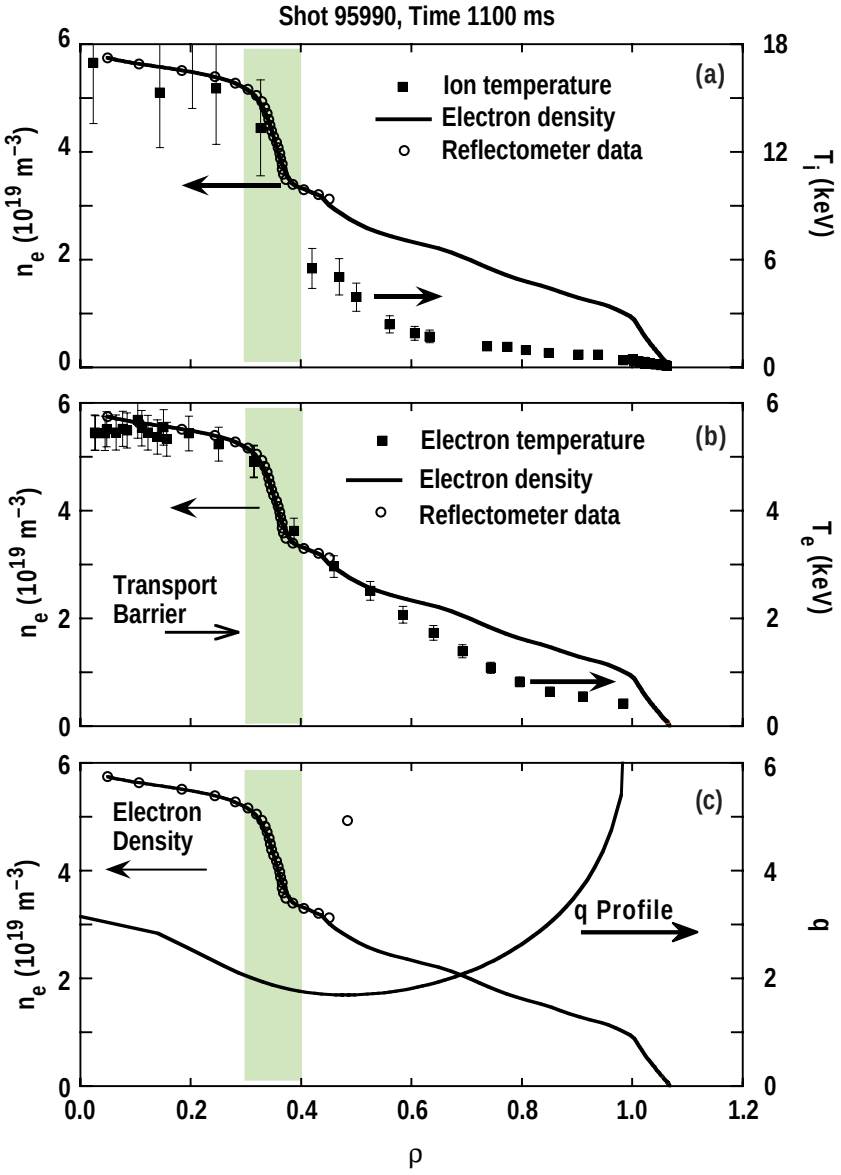

Fig. 1. Example of the spatial correlation of the particle, electron and ion thermal transport barriers observed on DIII–D. Profiles are shown for: (a) T_i, (b) T_e and, (c) the q profile, at 1.1 s in discharge 95990. The n_e profile is also plotted in each box (left hand scale). That portion of the n_e profile determined by the profile reflectometer system is indicated by the superimposed open circles.

cutoff by the increased electron density. However, if the profile volved as in the similar, but lower density, discharge illustrated in Fig. 1, then the T_e profile has steepened further by 1.5 s.

These results clearly demonstrate the different time scales for the formation of the ITBs in the four transport channels; the ion thermal and angular momentum channels track each other closely, while the particle and electron thermal channels also closely correspond (in this case), but develop after the ion and angular momentum ITBs. High levels of internal coherent mode activity in this discharge preclude accurate transport analysis. However, the abrupt, localized changes in profile gradients evident in Figs. 1 and 2 can be taken to correspond to localized changes in the transport coefficients, and indicate the formation of internal transport barriers. Profile gradients at the location of the core transport barriers are similar to, or exceed, those observed at the plasma edge during H–mode operation. For example, ∇T_i for the profile shown at 1.5 s in Fig. 2(a) has a maximum value of ~250 keV m^{-1}, which exceeds typical H–mode edge ∇T_i by a factor of 2–3, while L_{T_i} is short, ~5 cm. Finally, the conditions under which simultaneous ITBs are obtained closely correspond to conditions previously noted for obtaining electron thermal and particle transport barriers, i.e. strong NCS and (on DIII–D) $P_{NBI} \geq 8$ MW [5–9]. However, why localized, steep ITBs should sometimes be observed in the particle transport, but not electron thermal transport channel, and vice versa, and sometimes in all four transport channels simultaneously, is not fully understood.

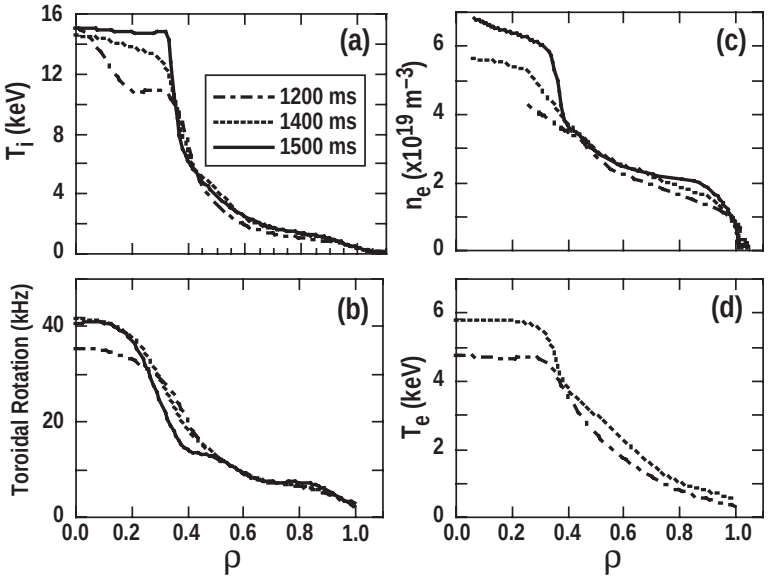

Fig. 2. Example of profile time evolution, illustrating differences in ITB development. Profiles are shown at 1.2 s (chain-dashed line), 1.4 s (dashed line) and 1.5 s (solid line) for: (a) T_i, (b) carbon toroidal rotation, (c) n_e and, (d) T_e, for discharge 95989.

III. Turbulence Characteristics

All improved transport regimes on DIII–D have been correlated with decreased local turbulence and turbulence induced transport [3], consistent with theoretical models of turbulence regulation via sheared **E**×**B** flows. In particular, core microturbulence is observed to decrease in NCS discharges, coincident with the first formation of ITBs [2]. In some of the highest performance discharges the core microturbulence is observed to decrease to the noise level of the FIR scattering and BES (beam emission spectroscopy) systems [2]. However, finite fluctuation levels are still present and detectable by the reflectometer systems on DIII–D. In the discharges shown in Figs. 1 and 2, the FIR scattering system indicates that core microturbulence is reduced, as in previous work. However, measurements with homodyne reflectometer channels indicate that the low-wavenumber (0 to ≥ 2 cm^{-1}) turbulence remaining after the formation of the core ion thermal and angular momentum transport barriers does not decrease during the subsequent formation of the very steep electron density and temperature profiles, in agreement with measurements on JT–60U [12]. As shown in Fig. 3(c), the frequency integrated rms level of the turbulence signal from a density layer of 4.4×10^{19} m^{-3} is essentially unchanged from shortly after 1.3 s, when the channel begins to reflect, until 1.5 s. Yet, as shown in Fig. 2(c) and (d), the n_e and T_e gradients steepen significantly during this time period; L_n, for example, changes from 28 cm at 1.4 s to 5 cm at 1.5 s. This suggests that the remaining low-wavenumber core turbulence is not driven by the evolving n_e and T_e profiles.

The level of **E**×**B** shear just inside the ITB location for the discharge shown in Fig. 3 is the second largest observed on DIII–D to date, and varies strongly with radius, yet the reflectometer turbulence signal is invariant as the probing density layer moves through varying levels of **E**×**B** shear. The high level of **E**×**B** shear is, however, consistent with the speculation, for which there is some evidence [6,7], that electron thermal transport may be governed by high-wavenumber ETG-type turbulence, suppression of which requires larger **E**×**B** shearing rates than for ITG modes [6,7]. A further challenge to theory is that linear stability calculations for the core plasma region inside the ITB frequently show no unstable modes [6,7], whereas finite residual turbulence is measured. Finally, also shown in Fig. 3(a) and (b) are edge D_α emission and an edge reflectometer signal, respectively. The edge reflectometer channel shows a characteristic decrease in turbulence signal [3] coincident with several transient periods of H–mode operation as denoted by the drops in the D_α emission. That the core channel does not respond to the changes in edge turbulence allows us to rule out contamination of the desired core O–mode signal by unwanted reflections from the edge X–mode layer, or contamination from the edge in general as an explanation for these results.

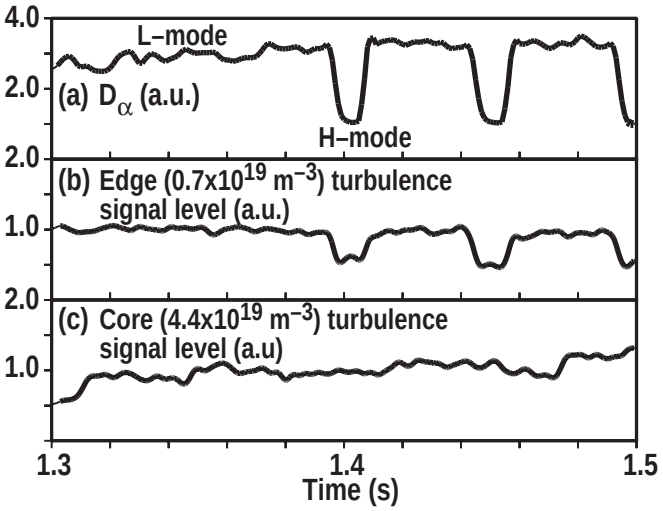

Fig. 3. Time evolution of: (a) divertor D_α emission, (b) frequency integrated rms turbulence signal level for an edge ($n_e = 0.7\times10^{19}$ m^{-3}) reflectometer channel and, (c) rms turbulence signal for a higher density ($n_e = 4.4\times10^{19}$ m^{-3}) core channel, for the same discharge illustrated in Fig. 2. The core signal remains essentially unchanged despite substantial steepening of the density profile during the period shown (L_n changes from 28 cm at 1.4 s to 5 cm at 1.5 s). By contrast, the edge turbulence signal shows a clear decrease at each of three L–H transitions.

This is a report of work supported by the U.S. Department of Energy under Grant Nos. DE-FG03-86ER53225, DE-FG02-89ER53296, and Contract Nos. DE-AC03-99ER54463 and W-7405-ENG-48.

[1] E.A. Lazarus, *et al.*, Phys. Rev. Lett. **77**, 2714 (1996).
[2] C.L. Rettig, *et al.*, Phys. Plasmas **5**, 1727 (1998).
[3] E.J. Doyle, *et al.*, in Fusion Energy 1996 (International Atomic Energy Agency, Vienna), Vol. I, p. 547 (1997).
[4] C.M. Greenfield, *et al.*, Phys. Plasmas **4**, 1596 (1997).
[5] K.H. Burrell, *et al.*, Plasma Phys. Control. Fusion **40**, 1585 (1998).
[6] C.M. Greenfield, *et al.*, 17th IAEA Fusion Energy Conf., Yokohama, Japan, 1998, to be published in Nucl. Fusion.
[7] B.W. Stallard, *et al.*, Phys. Plasmas **6**, 1978 (1999).
[8] B.W. Rice, *et al.*, Nucl. Fusion **36**, 1271 (1996).
[9] T. Fujita, *et al.*, Phys. Rev. Lett. **78**, 2377 (1997).
[10] E.J. Doyle, *et al.*, Rev. Sci. Instrum **70**, 1064 (1999).
[11] B. Bray, *et al.*, Bull. Am. Phys. Soc. **43,** 1892 (1998).
[12] R. Nazikian, *et al.*, 17th IAEA Fusion Energy Conf., Yokohama, Japan, 1998, to be published in Nucl. Fusion.